Isı Bilimi ve Tekniği Dergisi, 43, 1, 1-10, 2023
J. of Thermal Science and Technology
©2023 TIBTD Printed in Turkey
ISSN 1300-3615
https://doi.org/10.47480/isibted.1290659

NUMERICAL INVESTIGATION OF PLATE COOLING USING MULTIPLE IMPINGING JETS IN DIFFERENT ALIGNMENTS

Alperen YILDIZELI* and Sertac CADIRCI**
Department of Mechanical Engineering, Istanbul Technical University
34437 Gumussuyu, Istanbul, Turkey
*yildizeli@itu.edu.tr, ORCID: 0000-0002-1097-1359
**cadircis@itu.edu.tr, ORCID: 0000-0002-2281-721X

(Geliş Tarihi: 24.02.2022, Kabul Tarihi: 06.01.2023)

Abstract: In this study, convective heat transfer by multiple impinging jet arrays in different arrangements is numerically investigated using Computational Fluid Dynamics (CFD). Computational domain consists of multiple jet array either in inline or staggered alignment and a target plate to be cooled by impinging jets. Distance between the jet array and the target plate is kept constant at H=28 mm. Diameter of circular jet nozzles is fixed at D=5 mm for all configurations. Effects of jet Reynolds number (Re_j), spacing between circular jets and the alignment of the jet nozzles on aerothermal performance are parametrically investigated in the scope of this study. For staggered and inline alignments of the jet nozzles, Re_j ranges from 5000 to 20000 and the ratio of the spacing to the jet diameter (s/D) changes between 2 and 6. CFD calculations are performed using finite volume based ANSYS-Fluent flow solver. Simulations are conducted for incompressible, steady and turbulent flow using k-ω SST turbulence model with ideal gas assumption for density and Sutherland law for viscosity. After intensive mesh convergence and validation tests, appropriate mesh resolution is determined and parametric investigations are performed. The study reveals that most dominant parameter for plate cooling is Re_j followed by spacing between jets and finally jet alignment. For all Re_j, inline jet nozzle alignment provides 15% higher average heat transfer rate than staggered alignment when s/D is close to the lower limit. However, it is shown that jet alignment does not affect thermal performance when s/D is higher.
Keywords: Computational Fluid Dynamics (CFD), Multiple impinging jets, Heat transfer enhancement.

FARKLI DİZİLİMLERDE ÇOKLU ÇARPAN JETLER İLE PLAKA SOĞUTMASININ SAYISAL OLARAK İNCELEMESİ

Özet: Bu çalışmada, iki farklı dizilim ile konumlandırılmış çoklu çarpan jetler ile gerçekleştirilen taşınımla ısı transferi Hesaplamalı Akışkanlar Dinamiği (HAD) yöntemleri ile sayısal olarak incelenmiştir. Çözüm hacmi, hizalı veya şaşırtmalı olarak dizilmiş jetler, jet plakası, soğutulması hedeflenen plaka ve arada bulunan akış hacmini kapsamaktadır. Jet dizisi ile hedef plakası arasındaki mesafe H=28 mm olup, sabittir. Tüm dizilimlerde dairesel jet orifislerinin çapı sabit olup, D=5 mm'dir. Çalışma kapsamında jet Reynolds sayısının (Re_j), ardışık jetler arasındaki mesafenin ve jet orifisleri dizilim tipinin aerotermal performans üzerindeki etkileri parametrik olarak incelenmiştir. Jet orifislerinin şaşırtmalı ve hizalı dizildiği durumlar için, Re_j'nin 5000 ila 20000 arasında değiştiği ve ardışık orifisler arasındaki mesafenin orifis çapına oranının (s/D) 2 ila 6 arasında olduğu durumlar incelenmiştir. HAD hesaplamaları sonlu hacim yöntemi temelli ANSYS-Fluent akış çözücüsü kullanılarak yapılmıştır. Simülasyonlar sırasında, hal denklemleri için ideal gaz varsayımı ve viskozitenin sıcaklıkla değişimini ifade etmek için Sutherland yasası kullanılmıştır. HAD analizleri k-ω SST türbülans modeli kullanılarak sıkıştırılamaz, daimi ve türbülanslı akışlar için yapılmıştır. Çözüm ağından bağımsızlık ve doğrulama analizlerinin ardından uygun çözüm ağı belirlenmiş ve parametrik çalışmalar gerçekleştirilmiştir. Çalışma, hedef plakanın soğutulmasında en baskın parametrenin Re_j olduğunu, ardından jetler arasındaki mesafe ve son olarak jet dizilimi olduğunu ortaya koymaktadır. Jetlerin birbirine yakın olduğu durumlarda hizalı dizilimin, şaşırtmalı dizilime göre %15 civarında daha yüksek ısı transferi sağladığı görülmüştür. Buna karşılık ardışık jetlerin birbirinden uzak olduğu durumlarda hizalama tipinin ısıl performansına etkisinin görülmediği HAD analizleri ile ortaya konmuştur.
Anahtar Kelimler: Hesaplamalı Akışkanlar Dinamiği (HAD), Çoklu çarpan jet, Isı transferi iyileştirmesi.

NOMENCLATURE

D	Nozzle diameter [m]
E	Total energy [m^2/s^2]
HTU	Heat Transfer Uniformity [$=q''_{ave}/(q''_{max}- q''_{min})$]
k	Turbulence kinetic energy [m^2/s^2]
k_{eff}	Effective thermal conductivity [W/mK]
Nu	Nusselt number [$=hD/k_{eff}$]
PP	Pumping Power [W]
p	Pressure [Pa]
Re_j	Jet Reynolds number [$=\rho DV_{jet}/\mu$]
T	Temperature [K]
u	Velocity [m/s]

Greek symbols

η	Performance evaluation indicator [$=Nu^aHTU^b/PP^c$]
ρ	Density [kg/m^3]
ω	Turbulence specific dissipation rate [1/s]
μ	Dynamic viscosity [kg/ms]

INTRODUCTION

In most industrial applications cooling by forced convection with the consideration of cost-effective designs has become an urgent need over the last 30 years. In such applications, cooling by air is preferred since air can be widely found and cooling by air doesn't require precooling and exhaust air can be sent back to the atmosphere after filtering. Based on these advantages, air induced impinging jet cooling systems have become popular in many industrial applications and drawn the attention of researchers. Examples of cooling by multiple impinging jets in various industrial areas include blades' cooling in turbomachinery, electronics' cooling, quenching processes in glass and steel industries and air floatation dryers.

Chougule et al. (2011), investigated the effects of jet Reynolds number and distance between jets and plate on average Nusselt number in cooling by multiple impinging jets. They used a multiple impinging jet system consisting of nine jets in an inline arrangement and found that the k- ω -SST turbulence model predicted flow field and heat transfer rates more accurately than the other turbulence models. They revealed that the average Nusselt number increased with decreasing distance between jets and plate and increasing Rej. Wu et al. (2019), have investigated immersed impinging jet cooling system design for high-power electronics. For different air flow rates and temperatures, they conducted experiments to thermally characterize the cooling system in terms of Nusselt number. Additionally, they have conducted simulations and found compatible findings with their experimental results. Chen et al. (2020), have studied impinging jet cooling system in staggered configuration of jet nozzles. Roughness effects of the target plate were simulated with micro pin fins in the study. In addition to experiments, numerical simulations have been carried out. For different crossflow schemes, ribs were found to be effective on average Nusselt number while they were not effective as much on pressure losses. Finally, they found that the inline arrangement of jet nozzles results in higher thermal performance compared to the staggered alignment. Tepe (2021), has numerically investigated the effects of plate to target distance, nozzle spacing and Reynolds number on heat transfer performance of an impinging jet cooling system on a concave surface. After comprehensive verification studies, the k- ω SST turbulence model was chosen to be used for further simulations. Tepe (2021) found that with increasing plate to target distance and spacings, the average Nusselt number tends to decrease. In addition, spacing between sequential jets plays an important role in heat transfer uniformity. Zuckerman and Lior (2005) compared the performances of various turbulence models in the numerical modelling of multiple impinging jet flows. They compared the computational costs, and accuracies in heat transfer calculation and observed secondary Nusselt peaks in detail. In this study, the deviations of the turbulence models such as k-ε, k-ω, RSM (Reynolds Stress Model) and ASM (Algebraic Stress Model) from the experimental data are shown and the superiority of v2-f and k-ω SST turbulence models in predicting the flow field with high accuracy close to experiments have been highlighted. Obot and Trabold (1987) compared the effects of dominant parameters of the multiple impinging jet cooling system. They experimentally investigated the effects of three various jet to plate spacing ratios, Rej varying between 1000 and 21000, three crossflow schemes and jet to plate spacing ratios of 2 to 16. Based on the evaluation of measurements, low crossflow velocities and low jet to plate spacing ratios achieved enhanced heat transfer rates. Wen et al. (2018) investigated the effects of jet nozzle arrangement on heat transfer uniformity. In their study, they concluded that increasing the number of jets provided a uniform heat transfer distribution on the impinging plate and showed that varying the jet diameter in radial position increased the overall heat transfer. Chang and Shen (2019) investigated the effects of grooves on the impinging plate using two different web patterns along with the jet Reynolds, jet to plate distance and the jet diameter. They showed that heat transfer could be enhanced by using grooves and satisfying the conditions such as lower jet to plate distance than the jet diameter and moderate Rej ranging from 5000 to 20000. Vinze et al. (2019) experimentally investigated the effects of dimples on impinging plate on heat transfer in a multiple impinging jet cooling system at various jet Reynolds numbers, jet to plate distances, jet to jet spacing, dimple depths and eccentricities of dimples. They found that heat transfer enhancement could be achieved if the spacing between the jets was four times higher than the jet's diameter and dimples were used on the impinging plate. Xing and Weigand (2013) investigated the effect of the distance between the impinging plate and the jet array on heat transfer experimentally. At different impingement system

configurations, they examined an array consisting of 81 jets. They obtained Nu distribution on the surface by using the Thermochromic Liquid Cristal measurement technique and also solved one-dimensional time dependent heat transfer equation. In their study, they showed that for all impingement system configurations, higher thermal performance was achieved when the distance between the jet and the impinging plate was three times higher than the jet diameter. The thermal performance improvement provided by impinging jet systems has led researchers to utilize impinging jets for different perspectives in various application areas. Fu et. al (2021), investigated a novel application of impinging jet cooling for batteries of hybrid cars. They measured heat and momentum transfer of impinging jet cooling under cross-flow conditions created in a wind tunnel. They conducted CFD simulations based on k-ω SST turbulence model, compared numerical results with experiments and concluded that the vortex generation due to crossflow improves heat transfer. In their study, it was mentioned that the inlet jet pressure and jet height are also important parameters. Bijarchi et. al (2019), examined Swinging Sloth Impinging Jet (SSIJ) numerically. Parametric investigations were carried out with a 2D laminar model involving jet to plate distance, jet Reynolds number and the swinging frequency. The results showed that oscillation frequencies up to 10 Hz increase heat transfer by preventing boundary layer development. They also showed that, dimensionless jet to plate distances of 0.35 to 0.5 resulted in higher local Nusselt numbers. Sabato et. al (2019), numerically investigated the effect of different nozzle diameters and nozzle orientations on power electronic cooling utilizing impinging jet systems. Parametric simulations revealed that smaller nozzle diameters and inline arrangement showed better thermal performance. It has also been mentioned that required pumping power for impinging jet system is lower than for conventional power electronic cooling systems. Chauhan and Tankur (2014), developed a mathematical model for impinging jet solar air heaters and investigated the effects of Reynolds number, spanwise and streamwise distance between sequential jets and the diameter of jets on thermal efficiency. They concluded that, under certain operating conditions involving Reynolds number, impinging jet solar air heater shows higher thermal efficiency than the conventional design. The main challenge of industrial cooling applications is to maintain uniform and performant cooling with acceptable power requirements. Thus, the problem becomes a multi-objective industrial design problem. Consequently, the definition of those related parameters and a global performance evaluation become important to compare different configurations. In the current study, the cooling effect of multiple jets on an impinging plate with higher constant surface temperature is investigated numerically. To do this, the effects of the physical parameters such as jet Reynolds number and design parameters such as the spacing between the jets and jet's alignments on the heat transfer performance are examined. On a simplified cooling system, numerical simulations carried out with ANSYS Fluent provided a deep insight into the performance of various configurations based on heat transfer capabilities, heat transfer uniformity and finally energy consumption. As recent studies in the literature have shown, researchers have found different results from their studies due to the lack of overall evaluation parameters that include the necessary objective functions to indicate aero-thermal performance. The originality of the current study is based on the opportunity to select the appropriate design that meets the specific demands of industrial application. For this need, a performance evaluation indicator involving average Nu, heat transfer uniformity (HTU) and pumping power (PP) is defined which enables overall performance comparison between various designs.

METHODOLOGY

In this section, the problem of interest is introduced together with its computational domain and boundary conditions. The CFD approach and necessary mesh convergence tests and validation by experiments are explained in detail.

Computational Domain, Mesh and Boundary Conditions

Figures 1a and 1b show the computational domains for inline and staggered alignments, respectively. The model consists of a confinement wall with jet nozzles and a target plate placed opposite to it. The jet diameter, spacing between jet nozzles and the constant jet to plate distance are denoted by D, s and H, respectively. Several grid configurations consisting of tetrahedral and hexahedral elements are generated by ANSYS-Meshing and converted to polyhedral meshes in ANSYS-Fluent.

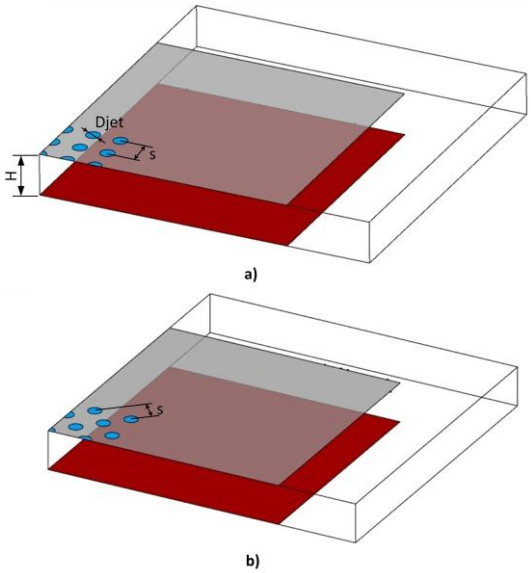

Figure 1. Computational Domains of: a) inline, b) staggered alignments.

The implemented boundary conditions are as follows: the plates are walls with no-slip boundary condition, the jet nozzles are prescribed with velocity inlet according to the jet Reynolds number and all lateral surfaces have pressure outlet. Thermal boundary conditions are as follows: constant temperature of 300.15 K is applied to each jet and the confinement wall, and the target plate is subjected to a constant temperature of 330.15 K. It should be pointed out that the geometric specifications of the impinging jet configurations such as the jet nozzle diameter D=5mm, jet to plate distance H=28mm, spacing ratios to the jet diameter 2 <s/D< 6 and the boundary conditions including the jet Reynolds number $5000<Re_j<20000$ are consistent with other studies.

Numerical Approach and Governing Equations

The CFD calculations have been carried out by finite-volume based flow solver ANSYS-Fluent. The continuity equation in Eq.(1), RANS equations in Eq.(2) and the energy equation in Eq.(3) together with transport equations for the k-ω SST turbulence model in Eq.(4) and Eq.(5) are solved numerically until their convergence criteria have been achieved. Readers may refer to (Menter, 1994) for details of the k-ω SST turbulence model. The Reynolds-averaged Navier-Stokes (RANS) equations in Eq.(1) and Eq.(2) show the same form as the instantaneous Navier-Stokes equations, but all the variables are ensemble-averaged, thus additional terms will appear that represent the effect of turbulence. These additional terms are the so-called Reynolds-stresses or turbulent-stresses associated with momentum fluctuations. In Eq.(2) they are represented by $(-\rho\overline{u_i' u_j'})$ and they have to be modeled in order to close Eq.(2). In the modeled energy equation in Eq.(3), E represents the total energy, k_{eff} is the effective thermal conductivity and $\left(\tau_{ij}\right)_{eff}$ is the deviatoric stress tensor. The SIMPLE algorithm was used with upwind schemes for all variables. The residuals to satisfy numerical convergence for continuity, momentum, turbulence and energy equations are determined as 10^{-3}, 10^{-4}, 10^{-4} and 10^{-6}, respectively.

$$\frac{\partial \rho}{\partial t} + \frac{\partial}{\partial x_i}(\rho u_i) = 0 \tag{1}$$

$$\frac{\partial}{\partial t}(\rho u_i) + \frac{\partial}{\partial x_j}(\rho u_i u_j) = -\frac{\partial p}{\partial x_i} + \frac{\partial}{\partial x_j}\left[\mu\left(\frac{\partial u_i}{\partial x_j} + \frac{\partial u_j}{\partial x_i} - \frac{2}{3}\delta_{ij}\frac{\partial u_l}{\partial x_l}\right)\right] + \frac{\partial}{\partial x_j}\left(-\rho\overline{u_i' u_j'}\right) \tag{2}$$

$$\frac{\partial}{\partial t}(\rho E) + \frac{\partial}{\partial x_i}\left(u_i\left(\rho E + p\right)\right) = \frac{\partial}{\partial x_j}\left(k_{eff}\frac{\partial T}{\partial x_j} + u_i\left(\tau_{ij}\right)_{eff}\right) + S_h \tag{3}$$

$$\frac{D\rho k}{\partial t} = \tau_{ij}\frac{\partial u_i}{\partial x_j} - \beta^*\rho\omega k + \frac{\partial}{\partial x_j}\left[\left(\mu + \sigma_k\mu_t\right)\frac{\partial k}{\partial x_j}\right] \tag{4}$$

$$\frac{D\rho\omega}{Dt} = \frac{\gamma}{\nu_t}\tau_{ij}\frac{\partial u_i}{\partial x_j} - \beta\rho\omega^2 + \frac{\partial}{\partial x_j}\left[\left(\mu + \sigma_\omega\mu_t\right)\frac{\partial \omega}{\partial x_j}\right] + 2(1-F_1)\frac{\rho\sigma_{\omega 2}}{\omega}\frac{\partial k}{\partial x_j}\frac{\partial \omega}{\partial x_j} \tag{5}$$

Air flow is assumed to be steady and incompressible with ideal gas and Sutherland law approaches in order to consider the changes of density and viscosity with respect to temperature for realistic predictions. Jet Reynolds number, local Nusselt number and area weighted average Nusselt number are given in Equations (6), (7) and (8), respectively.

$$Re_j = \frac{\rho V_{jet} D}{\mu} \tag{6}$$

$$Nu(x,y) = \frac{hD}{k_{eff}} = \frac{q''(x,y)D}{k_{eff}\left(T_{plate} - T_{jet}\right)} \tag{7}$$

$$\overline{Nu} = \frac{1}{A_{target,plate}}\int Nu(x,y)dA_{target,plate} \tag{8}$$

Thermal conductivity of air is taken as 0.02749 W/mK for Nusselt calculations which is in accordance with the temperature ranges of the case.

Turbulence Model

Different turbulence models that resolve wall vicinity have been compared in order to determine the appropriate turbulence model. Wall y^+ constraints have been considered to compare each turbulence model with proper mesh. Comparison of the numerical and experimental results is presented in Figure 2.

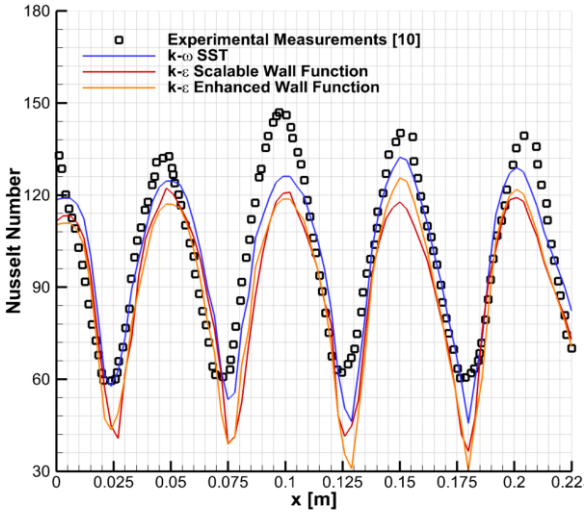

Figure 2. Turbulence model verification.

As can be seen from Figure 2, in accordance with other studies, the k-ω SST turbulence model was found to be in better agreement with the experimental data in the literature. Thus, the following studies were conducted with the k-ω SST turbulence model.

Mesh Convergence Tests and Validation Results

Before starting a comprehensive parametric investigation of the impinging jet configurations, intensive mesh convergence tests have been carried out to determine the adequate number of elements. The calculations were conducted according to the before-mentioned numerical approach and procedure with the same boundary conditions. Figure 3a indicates the local Nusselt number variation on the target plate for different number of elements and the comparison of the numerical results with the experimental data available in literature (Xing Y. and Weigand B., 2013). This validation study reveals that a mesh consisting of 4.6 million elements is found to be sufficient for further calculations. The deviations in the peaks of the Nu distribution along the plate are associated with the complexity of the impinging jet flow such as wash-up vortices and wall jet collision-separation that can be captured more accurately by numerical simulations rather than measurements. However, the average Nu does not change considerably in the mesh tests. Figure 3b supports this finding by showing that relative error in the average Nu converges as the number of elements increases.

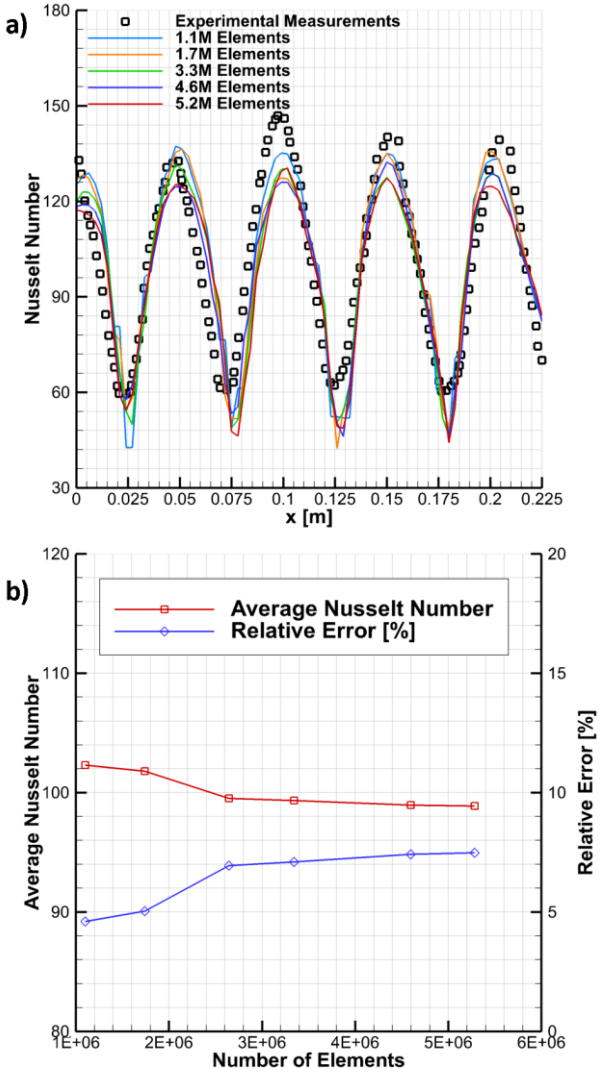

Figure 3. Results of mesh convergence tests a) Nu variation validated by experiments (Xing Y. and Weigand B., 2013) b) Mesh convergence summary

RESULTS

In this study, average Nu is considered as the objective function to examine the overall thermal performance of the impingement designs. Fig.4 shows the average Nu maps as a function of jet Reynolds number Re_j and s/D for inline and staggered alignments where there are 160 investigated cases in total.

In Figures 4a and 4b, it is obvious that Re_j is more dominant than the spacing between jets in enhancing forced convection. Increasing the Reynolds number affects both momentum and energy transfer positively which causes controversial results like increased demand for pumping power versus enhanced heat transfer. In the inline alignment, increasing s/D from 2 to 6 causes a relative 68% enhancement at all Re_j in cooling performance i.e. in average Nu. Distributing the jets to an extent up to six times of the jet diameter shows a %90 increase in average Nu values for staggered alignment. The effect of s/D can be associated with the peaks in the local Nu distribution as

demonstrated in Fig.3a, since uniformly distributed jets produce more cooling effect than jets close together.

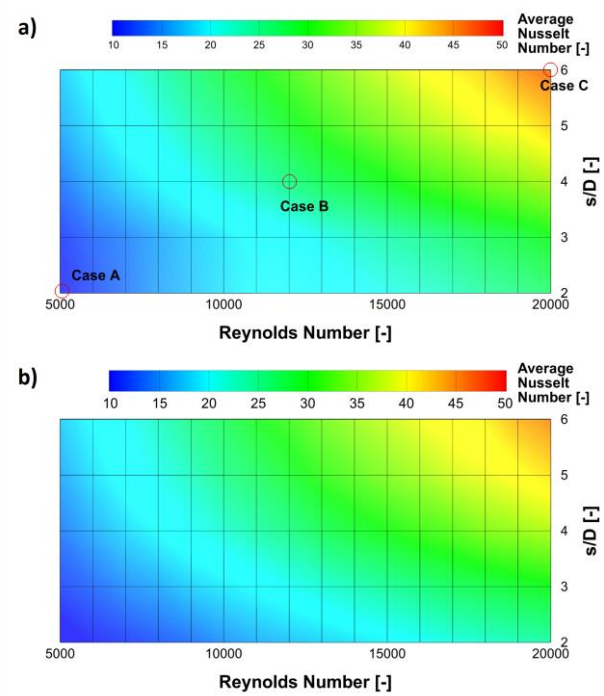

Figure 4. Average Nusselt maps for a) inline and b) staggered alignments, colours denote average Nu.

For inline and staggered alignments, increasing Re_j from 5000 to 20000 results in a relative 170% enhancement in cooling performance at all s/D ratios. When the performance of inline alignment is compared with the staggered one, overall averaged Nu values increased by 15% at s/D=2 for all Re_j. However, at higher s/D ratios, both configurations showed a 3% difference in overall averaged Nu for all Re_j. The influence of both alignments on the cooling performance is found to be remarkable at low s/D ratios rather than higher s/D ratios. Nevertheless, the alignment is always less significant than other parameters in terms of cooling performance. In accordance with the literature and Figure 4, it can be concluded that, jet Re as the flow attribute and s/D ratio as the main geometric design parameter affect overall Nu values on the target plate; indicating that, these two parameters have to be taken into consideration for forced convection applications utilizing impinging jets. Non-uniform cooling of materials causes large temperature gradients and thermal stresses which reduces the lifetime. Thus, cooling a material subjected to high temperatures uniformly is a major demand in most industrial applications involving thermal processes. In the current study, heat transfer uniformity has been taken into account and investigated as a target function depending on the parameters governing the cooling process. Heat transfer uniformity (HTU) is defined as the ratio of the average heat transfer rate to the difference between the maximum and minimum heat transfer rates as given in Eq.(9).

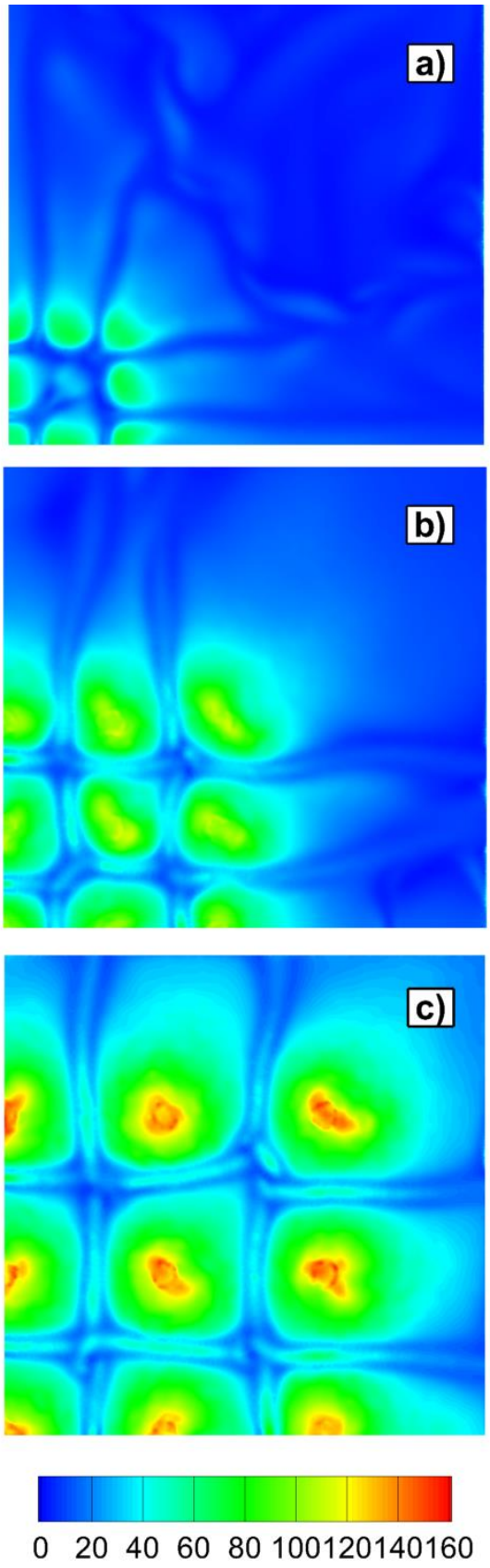

Figure 5. Surface Nusselt contours on target plate for three cases: a) Case A, b) Case B, c) Case C.

$$HTU = \frac{q''_{average}}{q''_{\max} - q''_{\min}} \quad (9)$$

Figure 5 demonstrates three representative individual cases selected from the design space for inline alignment. They are denoted by Case A, B and C and their local Nu contours on the target plate are shown in Fig. 5a, 5b and 5c, respectively. The corresponding cases have the specifications (Re_j;s/D)=(5000;2), (12000;4) and (20000;6), respectively. As it can be seen obviously, Case C has the highest Nusselt values at stagnation points and the lowest HTU value, in other words, the most uniformly distributed heat transfer is obtained in Case C among selected designs. Case A and Case B display that with decreasing Re_j and s/D, Nusselt peaks at stagnation points decrease as well as the average Nu and as a result, higher HTU values are observed which represents non-uniform cooling.

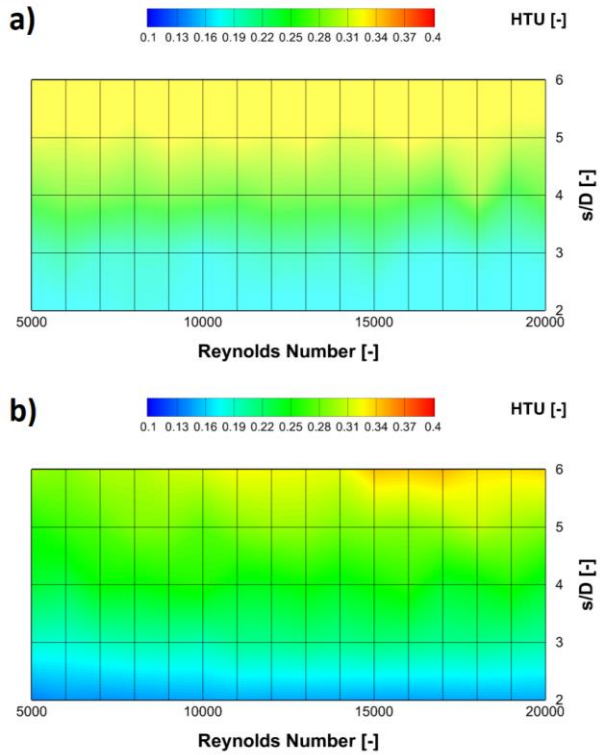

Figure 6. Heat transfer uniformity maps for a) inline and b) staggered alignments, colors denote HTU.

Figures 6a and 6b show heat transfer uniformity (HTU) maps on the design space for inline and staggered configurations, respectively. If HTU is investigated in order to evaluate uniform cooling, it should be pointed out that the alignment is a crucial factor acting on the capability of the impingement configuration. As it is shown in Figure 6, cooling the target plate is more uniformly achieved by inline alignment of the jet nozzles than by the staggered alignment. For the s/D value of two, inline alignment provides 30% to 40% higher HTU values. As s/D increases, the effect of alignment on heat transfer uniformity vanishes. For constant spacing, the effect of alignment on heat transfer uniformity is more dominant at lower Re values. In this respect, the s/D ratio maintains HTU more radically than the jet Reynolds number for the two alignments. In summary, increasing s/D to its upper limit supports uniform cooling performance at a lower HTU for both alignments. The power required to deliver jets to the impinging plate is calculated and plotted on the design space as shown in Fig.7. Eq.(10) shows the calculation of pumping power as the multiplication of pressure difference by the total volumetric flow rate of the jets Q. P_{inlet} and P_{outlet} denote the total pressures at the jet nozzle and pressure outlet, respectively.

$$PP = \left(P_{inlet} - P_{outlet}\right) Q \quad (10)$$

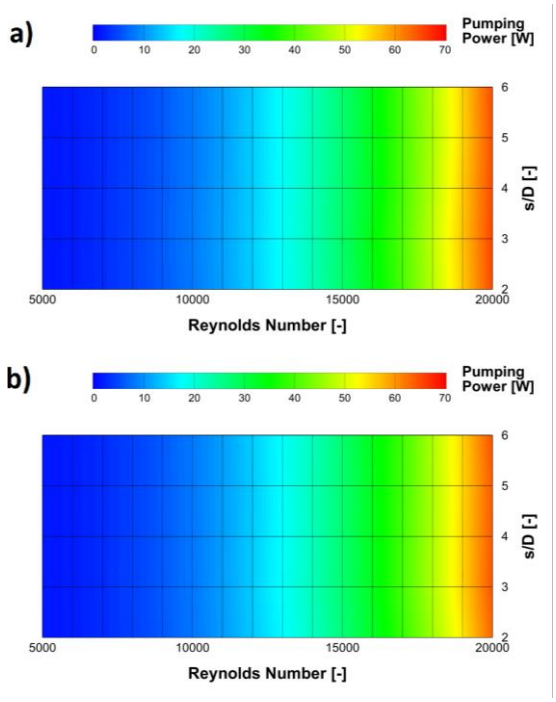

Figure 7. Pumping power results for a) inline and b) staggered alignments, colors denote pumping power

Since the power necessary for delivering air flow is directly related to the jet velocity, the pumping power strictly depends on the jet Reynolds number, hence it almost does not change with s/D. For two jet alignments, increasing Re_j from 5000 to 20000 considerably increases the pumping power which is necessary for corresponding cooling. As indicated in Fig.7, it was found out that the pumping power benefits from Re_j more than the average Nu in both configurations.

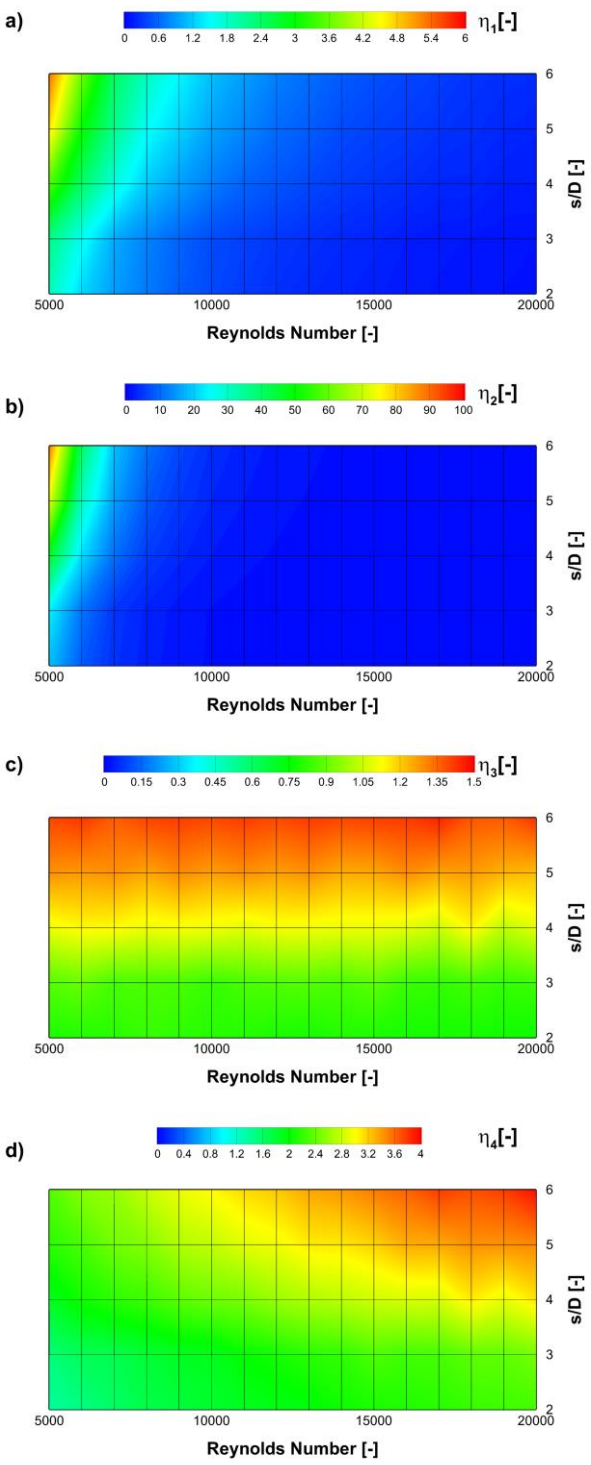

Figure 8. Performance evaluation indicator (η) maps for four different set of exponents a) a=b=c=1, b) a=2 b=1 c=2, c) a=0.4 b=0.7 c=0.1, d) a=0.5, b=0.5, c=0; colors denote η.

To evaluate the effects of each parameter for an overall comparison, performance evaluation indicator η in Eq.(11) was defined which depends on Nu, HTU and the pumping power. Suggested performance evaluation indicator reduces the multi objective decision making process consisting of three criteria into a single scalar by using weighted product method approach (Triantaphyllou, 2000). Performance evaluation indicator consist of constant a, b and c exponents for Nu, HTU and pumping power, respectively. Values of three exponents can be set in accordance with the importance of Nu, HTU and the pumping power for different applications. On the other hand, weighting of those constants has to be conducted by respecting the rule of the weighted product scalarization method where the condition (a+b-c=1) has to be satisfied. It should be pointed out that in Fig. 8 the graphics for η were obtained for four different configurations of arbitrary a,b and c exponents. Figures 8a and 8b show that the highest η values are obtained for the designs consisting of the highest s/D and lowest Re_j when overall heat transfer and energy consumption are prioritized as much as HTU. On the other hand, Figure 8c shows designs consisting of the highest s/D values become more preferable regardless of Re_j when HTU is more favourable than overall heat transfer and energy consumption. In Figure 8d, it can be seen that, designs with highest s/D together with highest Re_j become preferable when energy consumption is not regarded.

$$\eta = \frac{\overline{Nu}^{a} \times HTU^{b}}{PP^{c}} \tag{11}$$

CONCLUSION

In this study, forced convective heat transfer by impinging jets is investigated numerically for two different arrangements which are widely used in literature. The CFD calculations have been carried out by the flow solver ANSYS-Fluent with k-ω SST turbulence model for steady, incompressible air flow with ideal gas assumption and Sutherland law. In the current study, the problem has been investigated on the basis of the individual effects of the parameters on the objective functions rather than optimized solution and the results are evaluated for the whole design space. The CFD results reveal that jet Reynolds number is the most significant parameter in enhancing average Nu on the target plate followed by the spacing ratio to the jet diameter and finally alignment of the jet nozzles. The alignment of the jets nozzles is found to be insignificant in enhancing the cooling performance but can affect the uniformity of heat transfer. It is also shown that the pumping power remains almost the same for two alignments at all jet Reynolds numbers. In order to observe overall performance of different designs with a single indicator, overall heat transfer rate, required pumping power and heat transfer uniformity are combined into a single performance evaluation indicator by using weighted product method. It is shown that the suggested performance evaluation indicator provides a robust approach to determine optimum designs. By using suggested η indicators, one can suggest useful design points by selecting the a, b and c exponents based on the demands for different particular applications. In such applications, multi-objective optimizations should be integrated into the solution

procedure so that a balance is established for the aero-thermal demands.

REFERENCES

Bijarchi, M. A., Eghtesad, A., Afshin, H., and Shafii, M. B., 2019, Obtaining uniform cooling on a hot surface by a novel swinging slot impinging jet. Applied Thermal Engineering, 150, 781-790.
https://doi.org/10.1016/j.applthermaleng.2019.01.037

Chang S.W. and Shen H.D, 2019, Heat transfer of impinging jet array with web-patterned grooves on nozzle plate, International Journal of Heat and Mass Transfer, 141, 129–144.
https://doi.org/10.1016/j.ijheatmasstransfer.2019.06.048

Chauhan, R. and Thakur, N. S., 2014, Investigation of the thermohydraulic performance of impinging jet solar air heater, Energy, 68, 255-261.
doi.org/10.1016/j.energy.2014.02.059

Chen, L. and Brakmann, R. G., 2020, Detailed investigation of staggered jet impingement array cooling performance with cubic micro pin fin roughened target plate, Applied Thermal Engineering, 171, 115095.
doi.org/10.1016/j.applthermaleng.2020.115095

Chougule, N. K., Parishwad, G. V., Gore, P. R., Pagnis, S., and Sapali, S. N., 2011, CFD analysis of multi-jet air impingement on flat plate, Proceedings of the World Congress on Engineering 2011, London, United Kingdom.

Fu, J., Li, Y., Cao, Z., Sundén, B., Bao, J. and Xie, G., 2022, Effect of an impinging jet on the flow characteristics and thermal performance of mainstream in battery cooling of hybrid electric vehicles. International Journal of Heat and Mass Transfer, 183, 122206.
doi.org/10.1016/j.ijheatmasstransfer.2021.122206

Menter F.R., 1994, Two-Equation Eddy-Viscosity Turbulence Models for Engineering Applications, AIAA Journal, 32, 8.
doi.org/10.2514/3.12149

Obot N. T. and Trabold T. A., 1987, Impingement heat transfer within arrays of circular jets: Part 1—effects of minimum, intermediate, and complete crossflow for small and large spacings., Journal of Heat Transfer, 109, 872–879.
doi.org/ 10.1115/1.3248197

Sabato, M., Fregni, A., Stalio, E., Brusiani, F., Tranchero, M. and Baritaud, T., 2019, Numerical study of submerged impinging jets for power electronics cooling. International Journal of Heat and Mass Transfer, 141, 707-718.
doi.org/10.1016/j.ijheatmasstransfer.2019.06.081

Tepe, A.Ü., 2021, Numerical investigation of a novel jet hole design for staggered array jet impingement cooling on a semicircular concave surface, International Journal of Thermal Sciences, 162, 106792.
doi.org/10.1016/j.ijthermalsci.2020.106792

Triantaphyllou, E., 2000, Multi-criteria decision making methods: A comparative study. Springer, Boston, MA, 320-325.

Vinze, R., Khade, A., Kuntikana, P., Ravitej, M., Suresh, B., Kesavan, V., and Prabhu, S. V., 2019, Effect of dimple pitch and depth on jet impingement heat transfer over dimpled surface impinged by multiple jets, International Journal of Thermal Sciences, 145, 105974.
doi.org/10.1016/j.ijthermalsci.2019.105974

Wen, Z. X., He, Y. L., and Ma, Z., 2018, Effects of nozzle arrangement on uniformity of multiple impinging jets heat transfer in a fast cooling simulation device, Computers and Fluids, 164, 83-93.
doi.org/10.1016/j.compfluid.2017.05.012

Wu, R., Fan, Y., Hong, T., Zou, H., Hu, R., and Luo, X., 2019, An immersed jet array impingement cooling device with distributed returns for direct body liquid cooling of high power electronics, Applied Thermal Engineering, 162, 114259.
doi.org/10.1016/j.applthermaleng.2019.114259

Xing Y. and Weigand B., 2013, Optimum jet-to-plate spacing of inline impingement heat transfer for different crossflow schemes, Journal of Heat Transfer, 135, 7.
doi.org/10.1016/j.ijheatmasstransfer.2015.10.022

Zuckerman N. and Lior N., 2005, Impingement heat transfer: Correlations and numerical modeling, Journal of Heat Transfer, 127, 544–552.
doi.org/10.1115/1.186192